

Direct Observation of Kinetic Equation in Bubble Coarsening

Hiroshi Watanabe*

*The Institute for Solid State Physics, The University of Tokyo,
Kashiwanoha 5-1-5, Kashiwa, Chiba 277-8581, Japan*

Hajime Inaoka

*Advanced Institute for Computational Science, RIKEN, 7-1-26,
Minatojima-minami-machi, Chuo-ku, Kobe, Hyogo, 650-0047, Japan*

Nobuyasu Ito

*Department of Applied Physics, School of Engineering,
The University of Tokyo, Hongo, Bunkyo-ku, Tokyo 113-8656, Japan and
Advanced Institute for Computational Science, RIKEN, 7-1-26,
Minatojima-minami-machi, Chuo-ku, Kobe, Hyogo, 650-0047, Japan*

(Dated: March 6, 2019)

The coarsening behavior of bubbles is studied by molecular dynamics simulations. The kinetic equation, which denotes the growth or shrinkage rate of a bubble, is directly observed. In low temperature, the system exhibits $t^{1/2}$ law and the kinetic equation is well described by the classical Lifshitz-Slyozov-Wagner (LSW) theory for the reaction-limited case. This is the direct evidence that the bubble coarsening in low temperature is reaction-limited. In high temperature, while the system exhibits $t^{1/3}$ law which suggests that the system is diffusion-limited, the accuracy of the kinetic equations is insufficient to determine whether the form is consistent with the prediction of the LSW theory for the diffusion-limited case. The gas volume fraction dependence is also studied. While the behavior of the system in low temperature is less sensitive to the gas volume fraction up to 10%, that in high temperature deviates from the prediction of the LSW theory for the diffusion-limited as the gas volume fraction increases. These results show that the mean-field like treatment is valid for the reaction-limited system even with a finite volume fraction, while it becomes inappropriate for the diffusion-limited system since the classical LSW theory for the diffusion-limited case is valid for the dilute limit.

PACS numbers:

INTRODUCTION

When a thermodynamic variable, such as temperature or pressure, is quickly changed, a single phase system becomes unstable and the system is forced to put into a two-phase system. Then nucleation, growth, and coarsening are observed [1–3]. These phenomena are very common and widely observed in any systems involving the first-order transition. The coarsening, also termed Ostwald ripening, is the process that larger droplets of the second phase become larger at the expense of smaller ones in the ambient phase. There is a critical size in the system and droplets larger than it grow while smaller ones shrink. The basic theory of the coarsening was constructed by Lifshitz and Slyozov [4] and Wagner [5]. The theory is now referred to the LSW theory. The LSW theory predicts two typical behaviors in the diffusion-limited and the reaction-limited cases. The former is the limit where the diffusion process of the system is much slower than that of the reaction at the surface of droplets, where the reaction means dissolution/redeposition of droplets or evaporation/condensation of bubbles, etc. Assuming the self-similarity of the distribution function, the theory predicts that the asymptotic behavior of the critical radius is $t^{1/3}$ and it is called $t^{1/3}$ law. The other limit is the opposite case where the reaction process is much slower than that of the diffusion. Then the critical radius behaves as $t^{1/2}$ and it is called $t^{1/2}$ law. After the publication of the LSW theory, many experiments [6–9] as well as numerical simulations [10, 11] have been performed and the $t^{1/3}$ law was observed in most of them which suggests the diffusion-limited growth, while Koch *et al.* reported $t^{1/2}$ law in the isoenergetic system [10]. While the qualitative features of the LSW theory, such as the self-similarity of distribution functions or the power-law behavior of the characteristic length, have been confirmed, it is widely known that the form of a distribution function deviates from the prediction of the theory [12–15]. Since the original LSW theory is a kind of the mean-field theory, the many body effect is ignored and this approximation is justified for the dilute-limit, *i.e.*, the volume fraction of the second phase is negligible compared to the ambient phase. While considerable efforts have been made to extend the LSW theory to a system with a finite-volume fraction [16–21], relatively less attention has been paid to systems in the reaction-limited. Viswanatha *et al.* reported that the growth of ZnO is in between the

diffusion- and reaction-limited cases [9]. Rinaldo *et al.* considered the population dynamics of Pt and discussed the reaction-limited case. So far, most of the previous studies try to explain the macroscopic behavior of the system, such as the average size of droplets, by assuming the microscopic kinetics, namely, the form of the kinetic equation. Recently, Werz *et al.* investigates coarsening of particles in the Al-Cu system [22]. Owing to the improvements of the resolution of the X-ray tomography, they succeeded to track individual particles with submillimeter size, and determined the growth rate directly. They reported that the obtained growth rate, which is the kinetic equation, is significantly deviated from the prediction of the LSW theory.

In the previous study [23], we reported that the bubble coarsening in decompressed liquid exhibits the crossover from $t^{1/3}$ law to $t^{1/2}$ law as temperature increases. The exponents suggest that the system in low temperature is of the reaction-limited while it is of the diffusion-limited in high temperature. However, it is difficult to determine whether the microscopic dynamics are really determined by reaction or diffusion only from the macroscopic behavior such as the exponents of the average size of droplets, as pointed out by Viswanatha *et al.* [9]. Therefore, more detailed analyses are required to investigate the kinetics of bubbles. The purpose of the present paper is to investigate microscopic dynamics of bubble coarsening by observing the kinetic equation directly.

This paper is organized as follows. A brief summary of the theoretical background is given in Sec. . Section. is devoted to describe the method, especially how to determine the kinetic equation from the simulation data. The obtained results are presented in Sec. . Finally, Sec. concludes the present paper with discussions.

THEORY

Scaling Theory

We start from a distribution function $f(R, t)$ that denotes a number of bubbles having radius R at time t . We consider only a three-dimensional system for the simplicity, since a two-dimensional system involves logarithmic behavior [24, 25]. We assume that each bubble is a sphere, and its volume is given by $v = 4\pi R^3/3$. The time evolution of the system is governed by the following equation of continuity:

$$\frac{\partial f}{\partial t} = -\frac{\partial}{\partial R} (\dot{R}f), \quad (1)$$

where $\dot{R}(R, t)$ is the kinetic equation denoting the growth or shrinkage rate of a bubble having a radius R at time t . Here, we assume the mean-field like nature, *i.e.*, all bubbles in the system feel the identical ambient pressure. This assumption corresponds to the fact that the kinetic equation is single-valued. We also assume that the kinetic equation is a continuous function which means that there are no discontinuous jumps in volume of bubbles due to nucleation or coalescence. In the coarsening process, the critical radius $R_c(t)$ is defined where a bubble larger than the critical radius grows, while a bubble smaller than it shrinks. Following the manner of the LSW theory, we first assume the power-law behavior of the critical radius in the late stage of coarsening to be

$$R_c \sim t^\alpha, \quad (2)$$

with an exponent α . We introduce the scaling variable $\tilde{R} = R/R_c$, and assume the following asymptotic behaviors

$$f(R, t) \sim t^\beta \tilde{f}(\tilde{R}), \quad (3)$$

$$\frac{\dot{R}}{R_c} \sim t^\gamma \tilde{\dot{R}}(\tilde{R}), \quad (4)$$

with exponents β and γ . The total volume of the gas in this system V_G is

$$V_G \sim \int R^3 f dR = t^{\beta+4\alpha} \int \tilde{R}^3 \tilde{f} d\tilde{R}. \quad (5)$$

In the late stage of coarsening, the dynamics is dominated by the surface free energy, *i.e.*, the total surface area decreases while the total volume of gas is almost conserved. The conservation of the volume of gas leads to $\beta = -4\alpha$. Then we have the power-law behavior of the total number of bubbles $n(t)$ to be

$$n \equiv \int f dR = t^{-3\alpha} \int \tilde{f} d\tilde{R} \sim t^{-3\alpha}. \quad (6)$$

Requiring that the scaled functions are the solutions of Eq. (1), we have $\gamma = -1$. Therefore, there is only one exponent α which determines the dynamics of coarsening.

Equation (1) is rewritten with the scaled functions as

$$\alpha \left(4\tilde{f} + \frac{d\tilde{f}}{d\tilde{R}} \right) = \frac{d}{d\tilde{R}} \left(\tilde{R}\tilde{f} \right) \quad (7)$$

We rewrite Eq. (7) as,

$$3\tilde{f} = \frac{d}{d\tilde{R}} \left(u\tilde{f} \right), \quad (8)$$

where

$$u \equiv \left(\frac{\tilde{R}}{\alpha} - \tilde{R} \right). \quad (9)$$

Then Equation (7) is integrated to be [21]

$$\tilde{f} = \frac{1}{|u|} \exp \int_0^{\tilde{R}} \frac{3}{u} d\tilde{R}. \quad (10)$$

Equation (10) means that the distribution function f can be determined from the kinetic equation.

Kinetic Equations

Consider a growing bubble in bubble coarsening. When the bubble grows, two kinds of processes occur, a phase transition and a diffusion. The system exhibits two typical behaviors depending on which factor dominates the dynamics, the diffusion or the phase transition. In order that the bubble grows, atoms at the bubble surface should evaporate. Then the density of gas becomes higher than that of the center of the bubble. When the diffusion process is much slower than the evaporation rate, then the evaporation is always suppressed due to the high density at the surface. Then the diffusion determines the growing rate and this is referred to the diffusion-limited. On the other hand, if the evaporation rate is much slower than that of the diffusion process, then the gas density in the bubble is almost homogeneous and the dynamics are determined by evaporation rate. This case is referred to the reaction-limited. A kinetic equation, which denotes the growth/shrink rate of bubbles, has different form depending on whether the system is diffusion-limited or reaction-limited. [4, 5, 23, 26, 27]. Especially, Wagner discussed two cases, the diffusion-limited and the reaction-limited, simultaneously [5]. In this subsection, we give brief arguments of the kinetic equation of the bubble coarsening.

In the following, we assume that the system is in the hydrostatic equilibrium, *i.e.*, the Young-Laplace equation

$$\Delta P = \frac{2\sigma}{R}$$

is always satisfied, where ΔP is the pressure difference between inside and outside of a bubble, σ is the surface tension, R is the radius of the bubble, respectively. Note that, this is the static limit of the Rayleigh-Plesset equation which describes the inertial dynamics of a bubble. This approximation is justified when the time scale of pressure of liquid is much faster than the dynamics involved by chemical potential, such as diffusion or evaporation/condensation processes.

We consider a current J_R at the surface of a bubble. We assume that the system is spherically symmetric and the current is outward-pointing normal to the surface. The steady state solution is

$$J_R = \frac{D(\rho_R - \rho_0)}{R}, \quad (11)$$

where ρ_R is the density of gas at the bubble surface, D is a diffusion constant, and ρ_0 is a constant, respectively. If the system is diffusion-limited, *i.e.*, an evaporation/condensation rate is much faster than that of the diffusion process,

the gas density at the surface of the bubble equals to ρ_R^{eq} which is the equilibrium density at the surface of the bubble having a radius R . Then the growing rate of the bubble should be

$$\dot{v} = 4\pi R^2 J_R = 4\pi R D (\rho_R^{\text{eq}} - \rho_0), \quad (12)$$

with a constant ρ_0 . The linearized Gibbs-Thomson equation leads to

$$\rho_R^{\text{eq}} = \rho_\infty \left(1 - \frac{\lambda}{R}\right), \quad (13)$$

where ρ_∞ is the equilibrium density of gas at the flat surface and λ is the capillary length which is given by

$$\lambda = \frac{2\sigma V_m}{k_B T}, \quad (14)$$

where V_m is the molar volume, k_B is the boltzmann constant, and T is temperature, respectively. Putting Eq. (13) to Eq. (12), we have

$$\dot{v} \propto \left(\frac{R}{R_c} - 1\right). \quad (15)$$

Since $\dot{R}/R_c \sim t^{-1}\tilde{R}$, we have $\alpha = 1/3$, and therefore, $R_c \sim t^{1/3}$, which is called $t^{1/3}$ law.

Next, we consider the reaction-limited case. The evaporation/condensation rate is proportional to the difference between ρ_R^{eq} and ρ_R , when the difference is small. Then we have

$$\dot{v} = 4\pi R^2 k (\rho_R^{\text{eq}} - \rho_R), \quad (16)$$

with a proportional constant k . In the reaction-limited case, the diffusion current is virtually zero. Therefore, Eq. (11) leads to $\rho_R = \rho_0$. Considering Eq. (13), we have the kinetic equation as

$$\dot{v} \propto R \left(\frac{R}{R_c} - 1\right). \quad (17)$$

Since $\dot{R}/R_c \sim t^{-1}\tilde{R}$, we have $\alpha = 1/2$, and therefore, $R_c \sim t^{1/2}$, which is called $t^{1/2}$ law.

It is worth mentioning about the behavior of a kinetic equation in the limit of $R \rightarrow 0$. While the shrink rate remains finite in the diffusion limited case (15), it becomes zero in the reaction limited case (17). Therefore, if the shrink rate of a small bubble goes to zero, it is a strong evidence that the dynamics is of the reaction limited.

For later convenience, we introduce a scaling variable \tilde{v} as

$$\tilde{v} = \frac{v}{v_c}, \quad (18)$$

where $v_c \equiv 4\pi R_c^3/3$ is the critical volume and its asymptotic behavior is given by

$$v_c = v_0 t^{3\alpha}, \quad (19)$$

with a proportional constant v_0 . Then the kinetic equation for the reaction-limited case (17) is expressed to be

$$\dot{v} = K v_0^{1/3} t^{1/2} \tilde{v}^{1/3} \left(\tilde{v}^{1/3} - 1\right), \quad (20)$$

with a proportional constant K .

METHODS

We have performed molecular dynamics (MD) simulations with the truncated Lennard-Jones (LJ) potential. Refer the previous study for the details of the simulation [23]. In the following, we measure the physical quantities in the units of LJ, *i.e.*, the Boltzmann constant k_B is set to be unity, the length is measured by the diameter of atoms, and so forth. The system is a cube with linear size 960. The periodic boundary condition is taken in all directions. The time step is fixed to 0.005 throughout the simulations. The system is first thermalized to be the pure-liquid

T	N	ρ_i	c	ρ_e	ϕ
			1.025	0.712	0.04
0.8	678592512	0.767	1.05	0.663	0.08
			1.075	0.617	0.1
			1.025	0.570	0.04
1.0	542343168	0.613	1.05	0.530	0.06
			1.075	0.493	0.07

TABLE I: The conditions for simulations. The initial temperature T , the number of atoms N , the initial density ρ_i , the expansion rate c , the density after expansion ρ_e , and the volume fraction of gas ϕ are shown, respectively. All systems are cubes with the initial linear size 960 and expanded uniformly and adiabatically to be $c \times 960$.

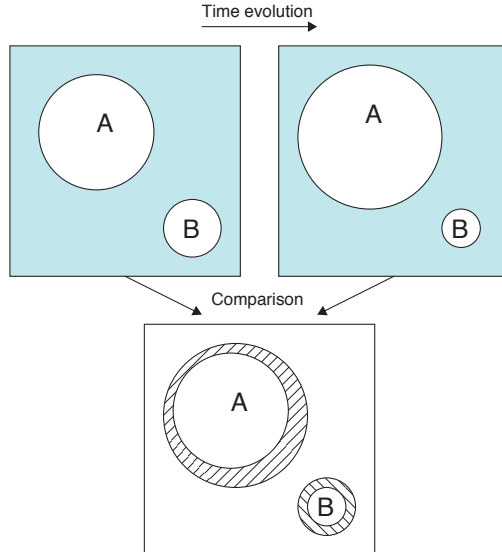


FIG. 1: A schematic illustration of the calculation of the kinetic equation. There are two successive snapshots. We first identify bubbles in each snapshot and then identify which bubble in a snapshot corresponds to which in the other one. In this example, two bubbles are found, A and B. After some time evolution, the bubble A grows while the bubble B shrinks. We can calculate the growth or shrinkage rates of them with the finite difference approximation.

phase using Nosé–Hoover thermostat [28]. The time evolution of the isothermal system is performed by the reversible reference system propagation algorithm (r-RESPA) [29]. We consider two initial temperatures, $T = 0.8$ and 1.0 . After thermalization of 10^4 steps, the thermostat is turned off and uniform and adiabatic expansion is performed. The linear size of the system is then changed from L to cL with an expansion rate c . The linear size of the system before expansion is set to be 960. We perform expansion with three values of the expansion rate $c = 1.025, 1.05$, and 1.075 . With larger values of c , the system is expanded strongly, which corresponds to deeper quench. The parameters used in simulations are summarized in Table. I. The initial density and the smallest value of the expansion rate are chosen so that the system after expansion becomes unstable and immediately exhibits a spinodal decomposition [30].

The snapshots of the system are stored every 1000 steps. After simulations, we identify bubbles for each snapshot on the basis of the subcell-dividing method [23, 30–32]. The system is divided into subcells and the local density is computed in each subcell. A subcell is identified to be in gas phase when its local density is lower than some threshold. Neighboring subcells in gas phase are identified to be a bubble. Since the densities of gas and liquid differ substantially, the identification process is robust against the value of the threshold. We choose the linear length of subcells to be about 3, which determines the resolution of bubbles' volume. Simulations were performed with a parallelized MD program [33, 34]. After expansion, the volume fraction of gas phase to liquid phase ϕ becomes almost constant during the coarsening. The values of ϕ are also shown in Table. I.

We calculated the growth or shrinkage rate of bubbles as follows. Consider two successive snapshots at time $t - \tau$ and $t + \tau$. First, we identify bubbles for each snapshot. If two bubbles have spatial overlap across two snapshots, then two bubbles are identified to be the same bubble (see Fig. 1). Suppose a bubble i has a volume v_i at time t . In

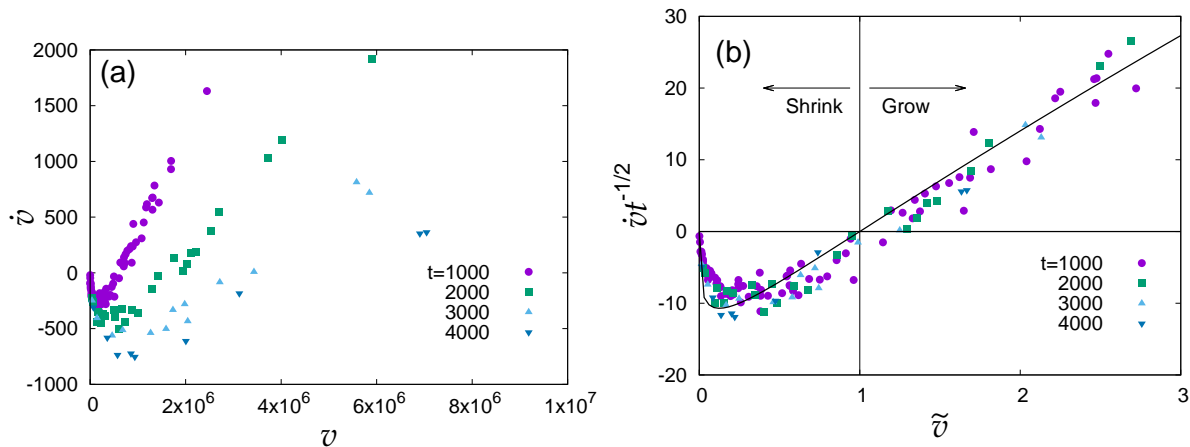


FIG. 2: (Color online) (a) Growth rates of bubbles at $t = 1000, 2000, 3000,$ and 4000 . Temperature is 0.8 and the gas fraction is $\phi = 0.04$. (b) A scaling plot of the kinetic equation. We assume $\alpha = 1/2$. The solid line denotes the theoretical prediction form described in Eq. (20) with $K = 16.8(4)$ and $v_0 = 16.7(3)$.

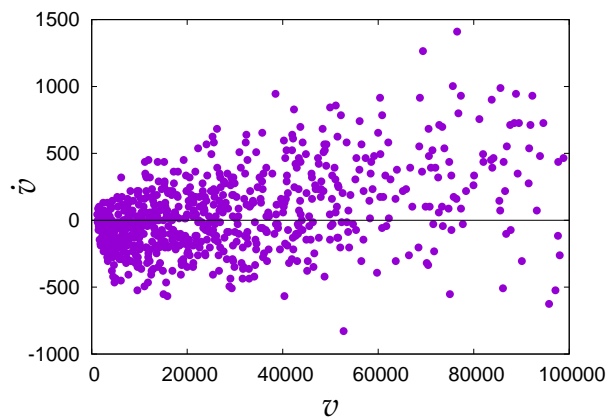


FIG. 3: Growth rates of bubbles at $t = 1000$ of the system with $T = 1.0$ and $\phi = 0.04$. It is difficult to determine whether the kinetic equation is of the form predicted in Eq. (15).

order to obtain the growth rate of the bubble, we adopt the central difference as

$$\dot{v}_i(t) \sim \frac{v_i(t + \tau) - v_i(t - \tau)}{2\tau}, \quad (21)$$

with a fixed time interval τ . In this simulation, we use $\tau = 5$. A pair of the volume and the growth rate ($v(t), \dot{v}(t)$) can be determined from a bubble in the snapshots. We calculate all growth rate of bubbles in a snapshot at time t . The set of growth rates is nothing but the kinetic equation.

RESULTS

Scaling Behavior of the kinetic term

The obtained kinetic equations for the case of $T = 0.8$ and $\phi = 0.04$ are shown in Fig. 2 (a). The kinetic equations are found to be almost single value functions. This fact means that bubbles feel the identical pressure at each time, and therefore, a mean-field like treatment is justified at this temperature. The scaling plot of the kinetic equations are shown in Fig. 2 (b). The kinetic equation at different time are well scaled with respect to the scaling variable \tilde{v} . One can also confirm that there is a critical volume $\tilde{v} = 1$, and growth rates of bubbles smaller than the critical size are negative, and therefore, the smaller bubbles shrink and vice versa. The solid line is the theoretical prediction in

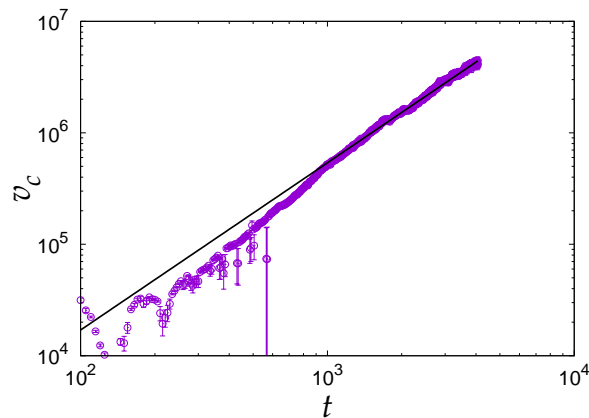


FIG. 4: (Color online) The time evolution of the critical volume at $T = 0.8$ and $\phi = 0.04$. Each point is obtained by fitting Eq. (20) to the data of the kinetic term. The errors of fitting are smaller than the size of symbols in most of points. The solid line is $v_0 t^{1.5}$ and the value of v_0 is estimated to be $17.02(3)$. The decimal logarithms are taken for both axes.

Eq. (20). There are two fitting parameters, K and v_0 , which are determined to be $16.8(4)$ and $16.7(3)$, respectively. The function form of the kinetic equation is well described by the prediction for the reaction-limited case (17), and clearly different from the form in the diffusion-limited case (15).

In the previous work, we observed the crossover from $t^{1/2}$ law to $t^{1/3}$ law as temperature increases [23]. Considering the value of exponent, the system in $T = 1.0$ is expected to be of the diffusion-limited case. However, we found that it is difficult to determine whether the kinetic equation has the form described in Eq. (15), as shown in Fig. 3

Critical Volume

Since the function form of the kinetic equation is well described by the theoretical prediction, we can estimate the critical volume at each time by fitting Eq. (20) to the obtained data. For fitting, we fix the value of the coefficient K to be 16.8 which is obtained by the scaling behavior of the kinetic equation. Therefore, the only fitting parameter is the critical volume $v_c(t)$ at each time t . The time evolution of the critical volume at $T = 0.8$ is shown in Fig. 4. In the scaling regime ($t > 10^3$), the critical volume is well described by the power-law behavior $t^{3\alpha}$ with $\alpha = 1/2$. Assuming Eq. (19), the coefficient of the critical volume is estimated to be $v_0 = 17.02(3)$ which is consistent with the value $v_0 = 16.7(3)$ obtained from the scaling behavior.

Distribution function

The kinetic equation (20) contains only two coefficients, K and v_0 . Since we have determined the value of them, we can reconstruct the distribution function using the relation in Eq. (10). The scaling behavior of the distribution function \tilde{f}_v and the cumulative distribution functions (CDFs) $F(\tilde{v})$ at $T = 0.8$ are shown in Fig. 5, where $\tilde{f}_v(\tilde{v}) \equiv 4\pi\tilde{R}^2$ is the distribution function of volume and $F(\tilde{v})$ is its CDF which is given by

$$F(\tilde{v}) = \int_0^{\tilde{v}} \tilde{f}_v d\tilde{v}. \quad (22)$$

While the CDF's are well scaled using the scaling variable \tilde{v} , the statistical precisions are insufficient to discuss whether the form of the distribution function deviates from the classical theory or not.

Gas volume fraction dependence

In this subsection, we consider the gas volume fraction ϕ dependence on coarsening behavior. Changing the strength of the expansion, we can control the gas volume fraction during coarsening. Since the initial temperature and density are fixed, larger values of ϕ corresponds to deeper quench. The temperature and the gas volume fraction dependence to

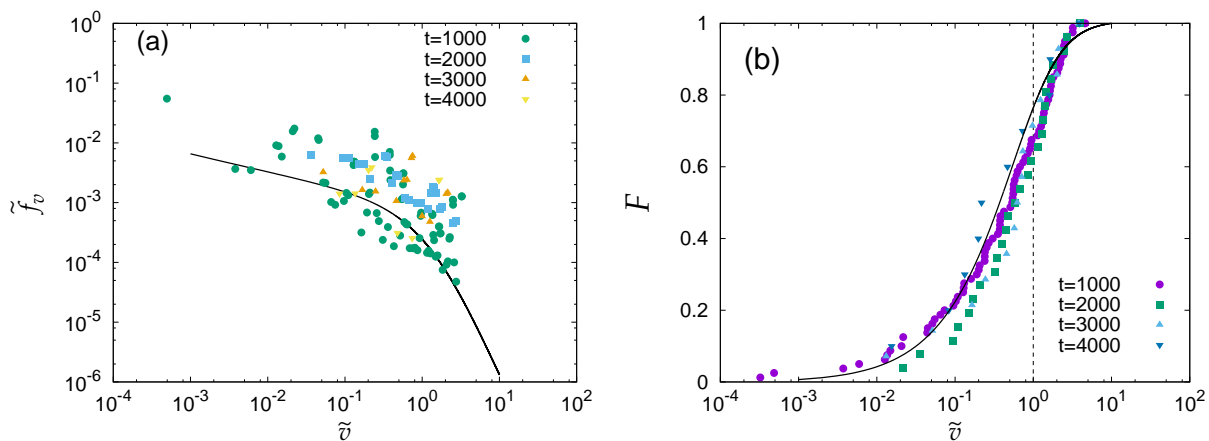


FIG. 5: (Color online) Scaling plots of (a) distribution functions \tilde{f}_v and (b) the cumulative distribution functions $F(\tilde{v})$. The data at $t = 1000, 2000, 3000,$ and 4000 are shown. The solid line denotes the reconstructed distribution function and the cumulative distribution function using the relation (10) with $K = 16.8$ and $v_0 = 17.02$. The decimal logarithm is taken for the both axes in (a) and for the horizontal axis in (b).

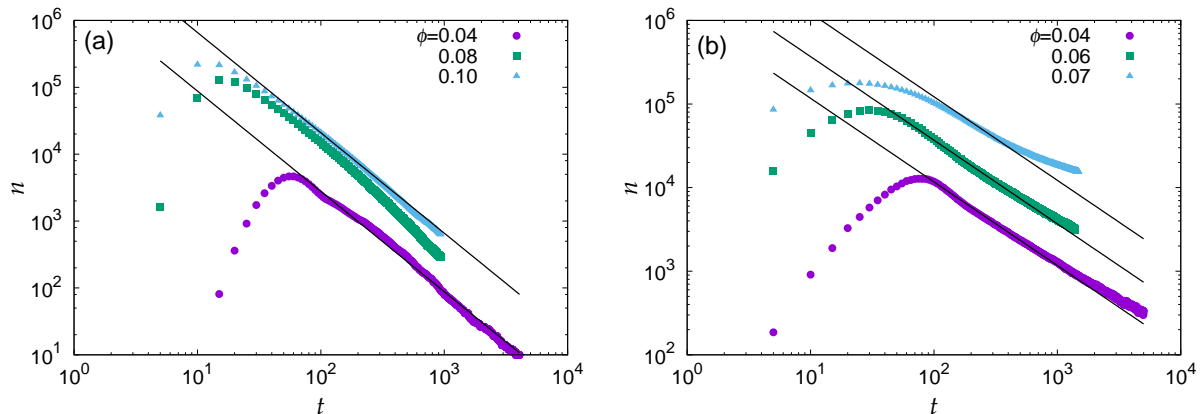


FIG. 6: (Color online) Time evolutions of the total number of bubbles. The decimal logarithm is taken for the both axes. (a) The data at the low temperature $T = 0.8$ cases. The solid lines $t^{-1.5}$ are used to guide to the eyes. (b) The data at the high temperature $T = 1.0$ cases. The solid lines t^{-1} are used to guide to the eyes. As the volume fraction of gas increases, the power-law behavior departs from the diffusion-limited case $n \sim t^{-1}$.

the time evolutions of the total number of bubbles are shown in Fig. 6. At the low temperature, the power-law behavior is found to be insensitive to the gas volume fraction. It is consistent to the fact that the system in low temperature is reaction-limited. If the system is reaction-limited, the dynamics is governed by the evaporation/condensation at the surface of bubbles, and therefore, the dynamics is less sensitive to the volume fraction of the second phase.

Meanwhile, the behavior at the high temperature is found to be sensitive to the gas volume fraction. While the power-law behavior of the total number of bubbles is well described by the diffusion-limited case $n \sim t^{-1}$, it departs from it as the volume fraction of gas increases. It is consistent to the fact that the system in high temperature is diffusion-limited. Since the classical LSW theory for the diffusion-limited case is justified only for the dilute-limit.

SUMMARY AND DISCUSSION

To summarize, we have performed the molecular simulations of bubble coarsening. We have observed both $t^{1/2}$ and $t^{1/3}$ laws which corresponds to the reaction-limited and the diffusion-limited cases of the LSW theory. From the time evolution of the bubble configurations, we have directly determined the kinetic equation of bubbles. In low temperature regime, the kinetic equation is consistent with the form predicted by the LSW theory for the reaction-

limited case. The scaling exponent is found to be less sensitive to the gas volume fraction up to 10%. These results are consistent with the LSW theory for the reaction-limited case. When the system is reaction-limited, the diffusion processes are almost negligible, the pressure of the ambient liquid is almost homogeneous, and the dynamics of bubble coarsening are determined only at the surfaces of the bubbles. Therefore, the mean-field like treatment is justified even for a finite volume fraction of the gas phase. While the scaling behaviors of CDFs and kinetic equations are well confirmed, the accuracy of the results is insufficient to discuss the shape of the form. This should be one of the further issues.

In high temperature regime, the total number of bubbles behaves as $n \sim t^{-1}$ which suggests that the system is diffusion-limited and the power-law behavior departs from it as the volume fraction of gas increases. These results are consistent with the fact that the classical LSW theory for the diffusion-limited case is valid for the dilute-limited.

With the help of the MD simulations involving about 10^8 atoms, we have up to 10^5 bubbles in the simulation box. However, the accuracy of the distribution function is insufficient for further analyses. While the kinetic equations in low temperature are determined with an acceptable accuracy, the accuracy of kinetic equations in high temperature is insufficient to determine whether the form is as predicted in the theory or not. Larger simulations are required to improve the accuracy.

Acknowledgements

The computations were carried out on the K computer provided by the RIKEN Advanced Institute for Computational Science through the HPCI System Research project (Project ID:hp130047) and on the facilities of the Supercomputer Center, Institute for Solid State Physics, University of Tokyo. We would like to thank H. Hayakawa and N. Kawashima for helpful comments. This work was supported by JSPS KAKENHI Grant Number 23740287 and 15K05201.

* Electronic address: hwatanabe@issp.u-tokyo.ac.jp; Corresponding author

- [1] J. Gunton, M. San Miguel, and P. Sahní, *Phase Transition and Critical Phenomena*, vol. 8 (Academic Press, London/New York, 1983).
- [2] J. D. Gunton and M. Droz, *Introduction to the theory of metastable and unstable states* (Springer-Verlag, Berlin/New York, 1983).
- [3] A. Onuki, *Phase transition dynamics* (Cambridge University Press, Cambridge, UK, 2002).
- [4] I. Lifshitz and V. Slyozov, *J. Phys. Chem. Solids* **19**, 35 (1961).
- [5] C. Wagner, *Z. Elektrochem.* **65**, 581 (1961).
- [6] X. Peng, J. Wickham, , and A. Alivisatos, *J. Am. Chem. Soc.* **120**, 5343 (1998).
- [7] G. Oskam, A. Nellore, P. R. L., , and P. Searson, *J. Phys. Chem. B* **107**, 1734 (2003).
- [8] Z. Hu, D. J. Escamilla Ramirez, B. E. Heredia Cervera, G. Oskam, and P. C. Searson, *J. Phys. Chem. B* **109**, 11209 (2005).
- [9] R. Viswanatha, P. K. Santra, C. Dasgupta, and D. D. Sarma, *Phys. Rev. Lett.* **98**, 255501 (2007).
- [10] S. W. Koch, R. C. Desai, and F. F. Abraham, *Phys. Rev. A* **27**, 2152 (1983).
- [11] R. Yamamoto and K. Nakanishi, *Phys. Rev. B* **49**, 14958 (1994).
- [12] P. Voorhees, *J. Stat. Phys.* **38**, 231 (1985).
- [13] M. Marder, *Phys. Rev. A* **36**, 858 (1987).
- [14] D. W. Oxtoby, *J. Phys.: Condens. Matter* **4**, 7627 (1992).
- [15] A. Baldan, *J. Mater. Sci.* **37**, 2171 (2002).
- [16] A. Brailsford, *J. Nucl. Materi.* **60**, 257 (1976).
- [17] M. Tokuyama and K. Kawazaki, *Physica A* **123**, 386 (1984).
- [18] P. Voorhees and M. Glicksman, *Acta Metall.* **32**, 2001 (1984).
- [19] P. Voorhees and M. Glicksman, *Acta Metall.* **32**, 2013 (1984).
- [20] Y. Enomoto, M. Tokuyama, and K. Kawasaki, *Acta Metall.* **34**, 2119 (1986).
- [21] L. Brown, *Acta Metall.* **37**, 71 (1989).
- [22] T. Werz, M. Baumann, U. Wolfram, and C. Krill, *Mater. Charact.* **90**, 185 (2014).
- [23] H. Watanabe, M. Suzuki, H. Inaoka, and N. Ito, *J. Chem. Phys.* **141**, 234703 (2014).
- [24] T. M. Rogers and R. C. Desai, *Phys. Rev. B* **39**, 11956 (1989).
- [25] J. H. Yao, K. R. Elder, H. Guo, and M. Grant, *Phys. Rev. B* **47**, 14110 (1993).
- [26] K. Binder, *Phys. Rev. B* **15**, 4425 (1977).
- [27] A. Bray, *Adv. Phys.* **43**, 357 (1994).
- [28] W. G. Hoover, *Phys. Rev. A* **31**, 1695 (1985).
- [29] M. Tuckerman, B. J. Berne, and G. J. Martyna, *J. Chem. Phys.* **97**, 1990 (1992).

- [30] H. Watanabe, M. Suzuki, and N. Ito, Phys. Rev. E **82**, 051604 (2010).
- [31] P. Warren, Phys. Rev. Lett. **87**, 225702 (2001).
- [32] H. Watanabe, M. Suzuki, and N. Ito, Comput. Phys. Commun. **184**, 2775 (2013).
- [33] H. Watanabe, M. Suzuki, and N. Ito, Prog. Theor. Phys. **126**, 203 (2011).
- [34] H. Watanabe, M. Suzuki, and N. Ito (2013), URL <http://mdacp.sourceforge.net/>.